frontiers in Earth Science

ORIGINAL RESEARCH
published: 12 April 2021
doi: 10.3389/feart.2021.631815

Sedimentary Responses to Climate Changes and Human Activities Over the Past 7400 Years in the Western Sunda Shelf

Kaikai Wu[1,2,3], Xuefa Shi[2,3], Zhanghua Lou[1]*, Bin Wu[2], Jingrui Li[3], Hui Zhang[2], Peng Cao[2] and Che Abd. Rahim Mohamed[4]*

[1] Ocean College, Zhejiang University, Zhoushan, China, [2] Key Laboratory of Marine Geology and Metallogeny, First Institute of Oceanography, Ministry of Natural Resources, Qingdao, China, [3] Laboratory for Marine Geology, Qingdao National Laboratory for Marine Science and Technology, Qingdao, China, [4] Faculty of Science and Technology, National University of Malaysia, Bangi, Malaysia

OPEN ACCESS

Edited by:
Min-Te Chen,
National Taiwan Ocean University, Taiwan

Reviewed by:
Nadia Solovieva,
University College London, United Kingdom
Pai-Sen Yu,
Taiwan Ocean Research Institute, Taiwan
Shiming Wan,
Institute of Oceanology, Chinese Academy of Sciences (CAS), China

***Correspondence:**
Xuefa Shi
xfshi@fio.org.cn
Zhanghua Lou
iwr@zju.edu.cn

Specialty section:
This article was submitted to Quaternary Science, Geomorphology and Paleoenvironment, a section of the journal Frontiers in Earth Science

Received: 21 November 2020
Accepted: 25 March 2021
Published: 12 April 2021

Citation:
Wu K, Shi X, Lou Z, Wu B, Li J, Zhang H, Cao P and Rahim Mohamed CA (2021) Sedimentary Responses to Climate Changes and Human Activities Over the Past 7400 Years in the Western Sunda Shelf. Front. Earth Sci. 9:631815. doi: 10.3389/feart.2021.631815

High-resolution records of grain size, major and trace elements, and Sr-Nd isotopes of Core K17 from the western Sunda Shelf were investigated to evaluate the response of weathering and terrigenous input to climatic changes and human activities over the past 7400 years. Sr-Nd isotopic results indicate that the Kelantan River is the main source of sedimentary material in the study core since the mid-Holocene. Chemical weathering levels are represented by the chemical index of alteration (CIA), $\alpha^{Al}Na$, and K_2O/Al_2O_3 ratios; and geochemical and grain size proxies (including TiO_2/CaO, Rb/Sr ratios, and grain size end-member) were used to establish variations of terrigenous input into the study core since 7400 cal yr BP. Based on these records, the evolution of weathering and terrigenous input processes in the western Sunda Shelf can be divided into four stages. During stage 1 (7400–3700 cal yr BP), increasing precipitation and decreasing temperature jointly balanced the relatively stable weathering and terrigenous sediment supply. Dramatically decreasing weathering rates were consistent with less rainfall and lower temperatures during stage 2 (3700–2600 cal yr BP). Heavy rainfall played a more important role than low temperature in controlling weathering and erosion, leading to increasing terrigenous input in stage 3 (2700–1600 cal yr BP). Because of the decoupling between weathering, erosion, and climate in the late Holocene (stage 4, since 1600 cal yr BP), increasing agriculture and related human activities likely dominated weathering and erosion relative to climate changes. Furthermore, the initial time at which human activity overwhelmed natural processes in the southern South China Sea (SCS) is similar to that in the northern SCS. Our results highlight that human activities during the past 1600 years have gradually overwhelmed natural climatic controls on weathering and erosion processes in the western Sunda Shelf.

Keywords: geochemistry, climate change, human activity, weathering, Sunda Shelf

INTRODUCTION

Continental weathering and erosion are critical processes controlling the delivery of sediments and solutes from the land to the ocean, shaping the terrestrial landscape, and regulating atmospheric CO_2 (Raymo and Ruddiman, 1992; Bi et al., 2015; Wan et al., 2015; Hu et al., 2020). Climate is a critical factor influencing weathering and erosion, because warm and humid conditions can typically enhance weathering intensity and erosion rates (White and Blum, 1995; West et al., 2005; Hu et al., 2020). Additionally, anthropogenic processes can alter landscapes and result in weathering and erosion pattern changes (Hu et al., 2013; Huang et al., 2018). Acquiring knowledge about the interactions between past climate, human activity, and weathering and erosion changes is important for comparing and understanding the present and future interactions among these systems (Huang et al., 2018).

Some studies on the interaction between climate change, human activities, and weathering and erosion have been performed in different locations in the northern South China Sea (SCS) regions and around the world (Corella et al., 2013; Hu et al., 2013; Wan et al., 2015; Huang et al., 2018). A general consensus is that human activities have dramatically influenced the natural environment and overwhelmed climate signals in sedimentary archives during the late Holocene (Wan et al., 2015; Huang et al., 2018). However, for the southern SCS, anthropogenic impacts have not been distinguished from natural variability in tropical Southeast Asia (Tan et al., 2019).

The Southeast Asia, located in tropical region, is characterized by intense rainfall and high temperatures that generally provide the highest global weathering and erosion rates (McLennan, 1993; Milliman et al., 1999; Liu et al., 2012), and thus it makes Southeast Asia a natural laboratory for studying the interactions between climate change, human activities, and weathering and erosion. As the largest low-latitude continental shelf, the Sunda Shelf is a huge sink of terrigenous sediments from rivers on surrounding regions due to its extremely low gradient (Hanebuth et al., 2011). Located in the central part of Southeast Asia, the Malay Peninsula yields and discharges large amounts of sediments by small mountainous rivers into the Sunda Shelf, up to ca. 35 Mt/yr (Liu et al., 2012), making the Peninsula an important provenance for the southern SCS region (Liu et al., 2016; Jiwarungrueangkul et al., 2019b; Wu et al., 2019). Moreover, the fluvial discharge in this region is largely influenced by the Asian–Australian monsoon, which influences rainfall and temperature through seasonal changes (Wang et al., 2011; Liu et al., 2012). Marine sediments record abundant environmental change signals during production, transportation, and deposition, including tectonics, climate, and human activities (Li et al., 2019). Studying the response of sedimentary records to rainfall and temperature in the western Sunda Shelf is of great significance for understanding the evolution characteristics of tropical monsoon in the geological history. Furthermore, the Sunda Shelf is located in the intersection of the Indian Ocean and the Pacific Ocean, and the ocean circulation system is very complex and interconnected, which is important for the study of the inter-oceanic material and energy cycle (Wu et al., 2020). Additionally, human activities, such as agriculture, began in peninsular Malaysia at least 2000 years ago (Liang et al., 2011) and influenced natural river sediment compositions and sediment yields (Kamarudin et al., 2015; Wang et al., 2017). Exploring long-term climate change and the impact of human activity on past weathering and erosion rates in the Peninsula will improve our understanding of landscape dynamics (Hu et al., 2020). High-resolution sedimentary archives from the western Sunda Shelf may shed light on the details of the complicated interaction of climate changes, human activities, and weathering and erosion in the Southeast Asia.

Numerous studies on the Sunda Shelf primarily focus on the impact of sea level change on sedimentary processes and biogeography evolution since the Last Glacial Maximum (Pelejero et al., 1999; Hanebuth et al., 2000, 2011; Voris, 2000; Steinke et al., 2003). Since ca. 7–8 ka, the coastline reached its modern position, and sea level was relatively stable with little fluctuation (Steinke et al., 2003); therefore, the impact of sea level on sedimentation was negligible. Estuary and coastal deposits formed when sea level was at its latest transgressional and highstand stages since 8 ka (Hanebuth et al., 2011; Zong et al., 2012). Thus, the estuary/coastal region is an ideal location to preserve records of regional erosion and weathering in the tropical Malay Peninsula influenced by climate change and human activities since the mid-Holocene on the western Sunda Shelf. However, well-preserved records for the middle and late Holocene in the western Sunda Shelf are scarce.

In this study, we present high-resolution grain size, major and trace element geochemistry, and Sr-Nd isotopes from Core K17 from the inner Sunda Shelf in the southern SCS. The primary objective is to evaluate sediment provenance and to explore the interactions between climate changes, human activities, and weathering and erosion on the western Sunda Shelf over the past 7400 years.

REGIONAL SETTING

The Kelantan River, located in the northeastern Malay Peninsula (**Figure 1B**), is the second largest river on the Peninsula with a length of 335 km and flows from south to north into the SCS. It originates from the "Main Range" of the peninsular Malaysia near Gunong Korbu at an elevation of approximately 2100 m, and its gradient drops less than 100 m over the last 100 km (Koopmans, 1972). The river has a drainage area of 12,691 km^2, mean annual rainfall of 2500 mm, mean annual runoff of 1500 mm, and mean sediment load of 13.9×10^6 t (Liu et al., 2012; **Table 1**). Principal surrounding rivers include the Chao Phraya (Thailand), Mekong (Indochina Peninsula), and Pahang (peninsular Malaysia).

As a part of Sundaland, peninsular Malaysia has been tectonically stable since the Mesozoic, with few strong tectonic activities (Hutchison, 1968). Topographically, 90% of the coastal plain is less than 75 m above mean sea level. Most river drainage is covered by Quaternary alluvium; the Mesozoic granites underlie the alluvial coastal plain and outcrop on both sides of the Kelantan River Valley (Awadalla and Noor, 1991).

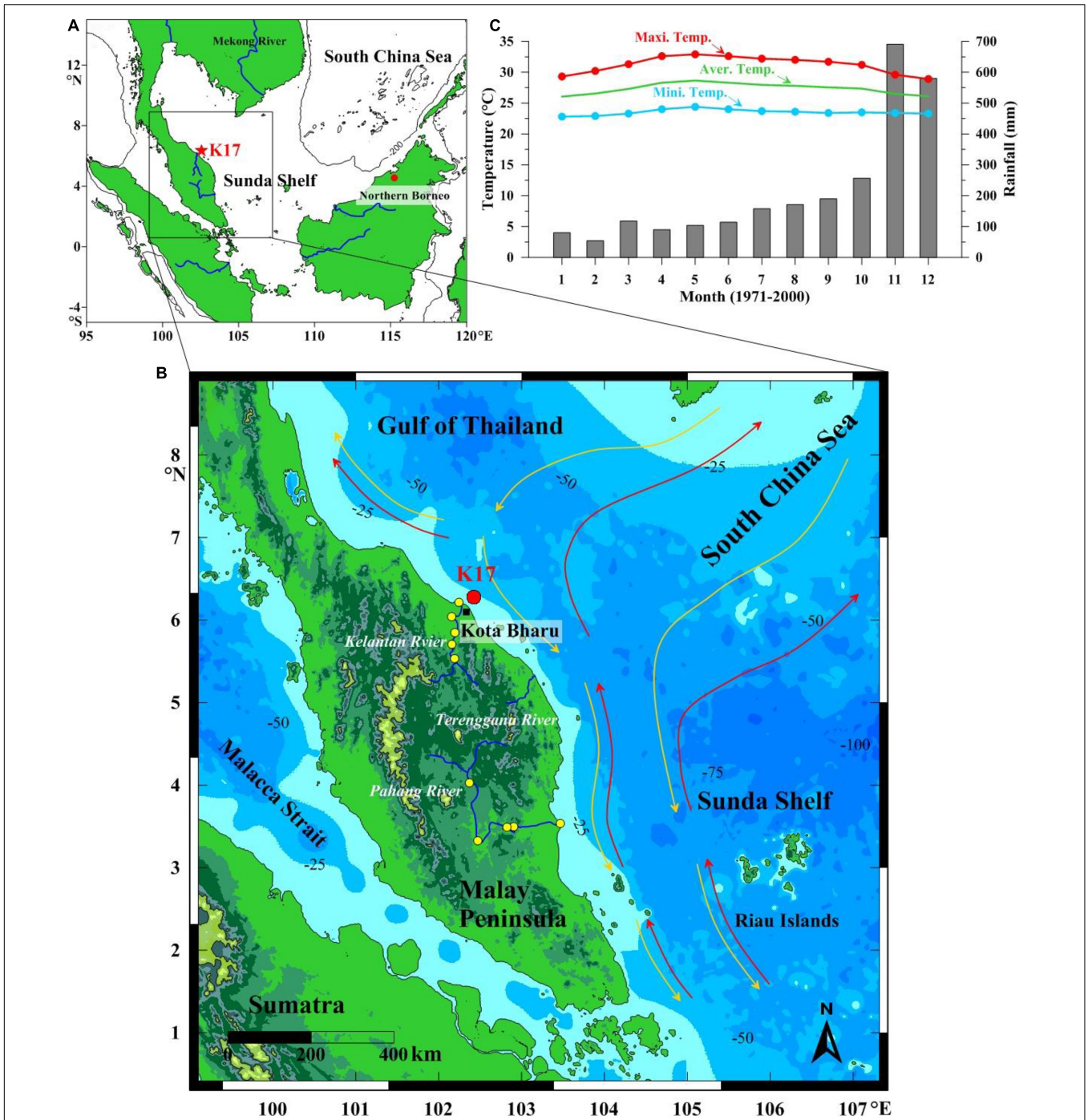

FIGURE 1 | (A) Locations of K17 (red star) and paleoclimate records from stalagmites (red dots) referenced in the text: Northern Borneo (Partin et al., 2007). **(B)** Geographic setting and prevalent hydrography of the western Sunda Shelf. Hydrography was modified from Tangang et al. (2011). The red and yellow arrows show the southwest and northeast monsoon currents, respectively. The locations of Core K17 and Sr-Nd sites of Kelantan and Pahang rivers are exhibited by red dot and yellow dots, respectively. **(C)** Regional monthly average precipitation (gray bars) and temperature over Kota Bharu from 1971 to 2000. Temperature and rainfall data are from the World Weather Information Service (http://www.worldweather.org).

Various types of Paleozoic sedimentary and metamorphic rocks are found between the eastern and western granitic masses. Shale and quartzite are the predominant sedimentary rock types (Awadalla and Noor, 1991).

The climate in peninsular Malaysia is controlled by the East Asian–Australian monsoon (Wang et al., 2005, 2011; Liu et al., 2012) with small seasonal temperature variations (**Figure 1C**) but substantially different characteristics between

TABLE 1 | Basic information of main rivers drained into the western Sunda Shelf (Liu et al., 2012, 2016).

River name	Length (km)	Annual rainfall (mm)	Drainage area (km^2)	Annual runoff (mm/year)	Suspended sediment discharge (Mt/year)
Kelantan River	280	875	12,691	1500	13.9
Pahang River	459	2170	29,300	947	20.4
Mekong River	4180	1570	790,000	590	160
Chao Phraya River	1252	1487.3	160,000	188	11

the wet and dry seasons (Wang et al., 2011). From October to January, the region is controlled by the southwesterly East Asian monsoon and receives abundant rainfall (the wet season) (**Figure 1C**). In other periods, the river basin is controlled by the northeasterly Australian monsoon, and the weather is relatively dry with less precipitation (the dry season) (Liu et al., 2012).

The water depth of the Kelantan River estuary ranges from 5 to 25 m, and the slope of the sea floor adjacent to the estuary is extremely gentle. Furthermore, the surface circulation in the southern SCS is primarily controlled by the monsoon (Tangang et al., 2011; **Figure 1B**). The entire southern SCS experiences cyclonic circulation during the northeast monsoon period (winter), whereas the surface current direction is opposite during the southwest monsoon period (summer) (Tangang et al., 2011). Tides are irregular with diurnal to semidiurnal tides (1.5:1). The mean spring range and maximum tidal range are 0.6 and 1.2 m, respectively (Raj et al., 2007).

MATERIALS AND METHODS

Materials

The gravity Core K17 (6.2°N, 102.34°E; 133 cm) was collected at a water depth of 11.4 m on the Kelantan River estuary of the northeastern Malay Peninsula during the R.V. DISCOVERY cruise in 2017 (**Figure 1**). The lithology of Core K17 is primarily olive gray homogeneous silt and sandy silt in the upper 10 cm (**Figure 2**). The lower section from a depth of 10–50 cm is composed of olive gray and dark greenish interlaid sandy silt with a 6 cm thick high sand and a biological debris layer between depths of 36 and 42 cm; below 42 cm to the base, the core primarily consists of dark greenish gray homogeneous sandy

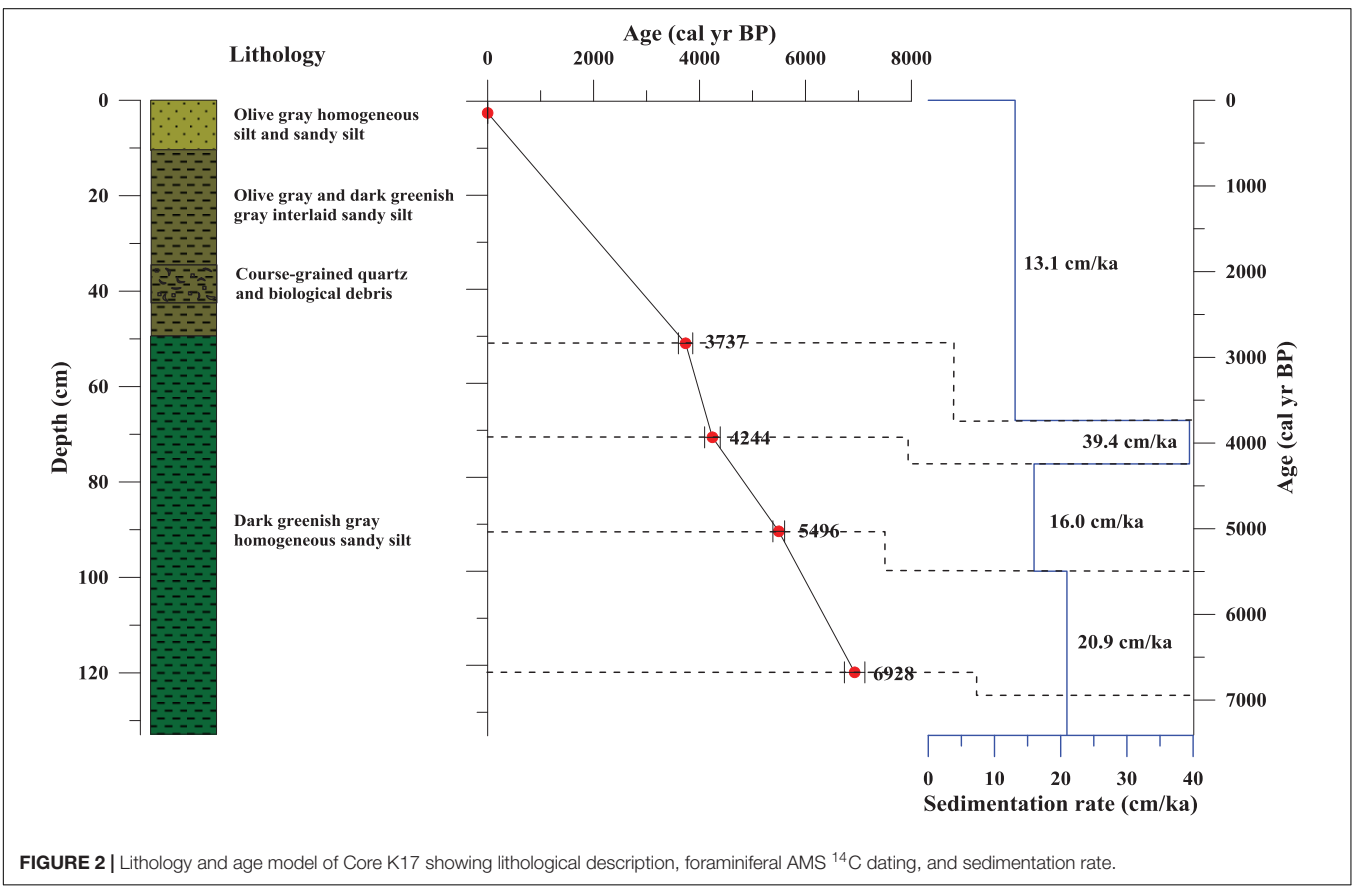

FIGURE 2 | Lithology and age model of Core K17 showing lithological description, foraminiferal AMS ^{14}C dating, and sedimentation rate.

silt (42–133 cm). A total of 132 samples were subsampled at 1 cm intervals for grain size, geochemical elements, and Sr-Nd isotope analyses.

AMS^{14}C Analyses

The chronology of Core K17 was established using AMS^{14}C data (**Figure 2** and **Table 2**). Because of the estuarial location and low carbonate content (<10%), there were few planktonic foraminifera. We picked more than 4 mg of mixed benthic foraminiferal species for five samples from the core. The raw radiocarbon ages were corrected for a local reservoir age of −15 ± 38 years (Southon et al., 2002) and converted to calendar ages using Calib Rev 7.0.4 (Reimer et al., 2013). The AMS^{14}C dating was performed at the Beta Analytic Laboratory, United States.

Grain Size Analyses

The grain size distribution of 132 samples of Core K17 was determined using a Malvern 2000 Mastersizer Particle Size Analyzer with a measurement range and resolution of 0.02–2000 μm and 0.01 Φ, respectively, at the First Institute of Oceanography (FIO), Ministry of Natural Resources (MNR), Qingdao, China. Bulk sediments were treated with an excess of 30% H_2O_2 and 3 mol/L HCl for 24 h at 25°C to remove organic matter and carbonates, respectively. Then, the samples were washed with distilled water until excessive H_2O_2 and HCl were completely removed before measurement. The relative error of the repeated measurements was less than 3%.

Geochemical Element Analyses

The geochemical element concentrations of 122 samples of Core K17 were analyzed using inductively coupled plasma optical emission spectrometry (ICP-OES; SiO_2, Al_2O_3, K_2O, Na_2O, Fe_2O_3, TiO_2, MgO, CaO, P_2O_5, MnO, and Sr) and inductively coupled plasma-mass spectrometry (ICP-MS; Rb, Cu, and Pb) at FIO. Approximately 50 mg of ground bulk sediment was digested with ultrapure HNO_3 and HF (1:1) in a Teflon digestion tank at 195°C for 48 h before measurement (Li et al., 2019). The standard material GSD-9 was assessed once after every 10 samples to provide quality control of accuracy and precision, and the relative standard deviations of analyzed elements were less than 5%.

Sr-Nd Isotope Analyses

The Sr and Nd isotopes of 10 decarbonated samples of Core K17 were determined using a Thermo Scientific multi-collector-inductively coupled plasma-mass spectrometer (MC-ICP-MS Nu plasma) at FIO. The samples were decarbonated using 0.25 N acetic acid and centrifuged and rinsed three times using Milli-Q purified water to eliminate traces of the carbonate fraction. Subsequently, the samples were completely dissolved in a HF–HNO_3–$HClO_4$ mixture (Li et al., 2018). Sr and Nd isotopes were extracted from the solution using a standard ion-exchange procedure. $^{88}Sr/^{86}Sr$ = 0.1194 and $^{146}Nd/^{144}Nd$ = 0.7219 were adopted to calibrate the mass bias during the Sr and Nd isotope measurements, respectively. Repeated analyses of the NBS987 standard yielded $^{87}Sr/^{86}Sr$ = 0.71031 ± 0.00000777 (1σ), and the JNdi-1 standard yielded $^{143}Nd/^{144}Nd$ = 0.512115 ± 0.00000556 (1σ), which is well within the recommended range.

RESULTS

Chronological Framework

The ages of this downcore were calculated by linear interpolation among five dated sediment layers, and the basal age was 7400 cal yr BP (**Figure 2**), which was calculated by linear extension after 6298 cal yr BP based on the same sedimentary rate with upper section under similar sedimentary environment. The ages were reported in years before present (yr BP). The linear sedimentation rates vary in the range of 13–39 cm/ka, with an average of 18 cm/ka (**Figure 2**). The sedimentation rates of the Middle Holocene (average 22 cm/ka) were relatively higher than those during the Late Holocene (average 13 cm/ka), and the highest sedimentation rate occurred during 3700–4200 cal yr BP, with a value of 39 cm/ka. The average time resolution of Core K17 was 56 yr/cm.

Grain Size Compositions and End-Member Extraction

The sediment fractions of the studied core are primarily silt (37–82%), with a secondary amount of sand (5–51%) and clay (4–25%) (**Figure 3**). According to Folk's classification (Folk et al., 1970), the sediment types are characterized by sandy silt, similar to the western Sunda Shelf (Wu et al., 2020). The mean grain size (Mz) of this downcore ranges from 3.4 to 6.8 Φ (average of 5.4 Φ). The sorting coefficient varies from 1.3 to 3.2, which is classified as poorly sorted. The mean grain size and sorting coefficient show a sudden increase of approximately 2900 cal yr BP (**Figure 3**).

TABLE 2 | AMS^{14}C dating age model of Core K17.

Depth (cm)	Sample ID	Sample material	Conventional AMS^{14}C age (yr BP)	Calendar age (cal yr BP)	Depth interval (cm)	Sedimentation rates (cm/ka)
2-3	Beta-505054	Foraminifera	103.55 ± 0.39 pMC	0	0–2.5	0
51-52	Beta-505056	Foraminifera	3780 ± 30	3737	2.5–51.5	13.1
71-72	Beta-505057	Foraminifera	4150 ± 30	4244	51.5–71.5	39.4
91-92	Beta-505058	Foraminifera	5130 ± 30	5496	71.5–91.5	16.0
121-122	Beta-505060	Foraminifera	6410 ± 60	6928	91.5–121.5	20.9

pMC, percent modern carbon.

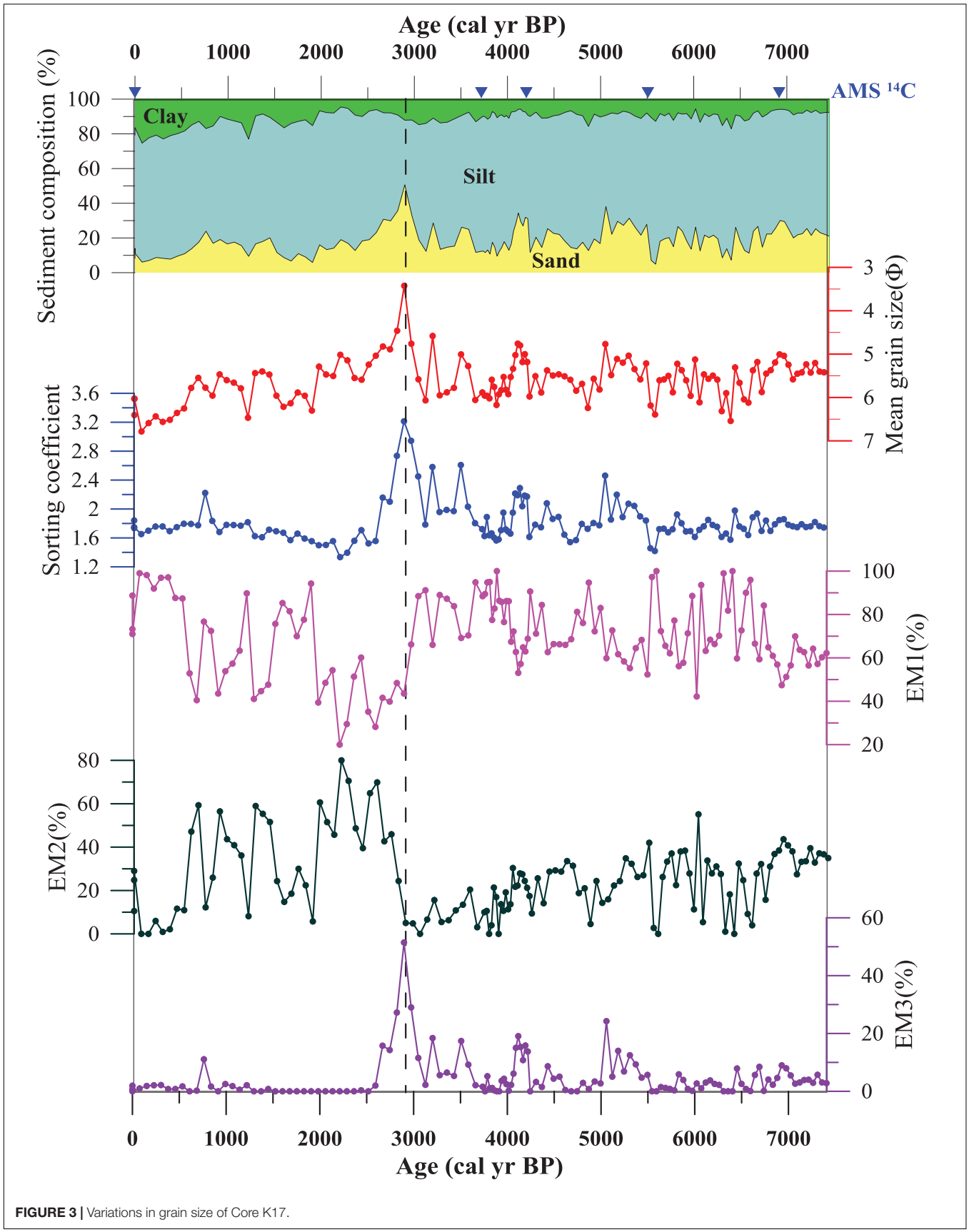

FIGURE 3 | Variations in grain size of Core K17.

An inversion algorithm was used to extract grain size end-members (Joussain et al., 2016; Li et al., 2019), and the results display a three-end-member model that explains more than 95% of the variance (**Figure 4A**). The fine end-member EM1 varies widely range of −0.9 to 10.4 Φ and explains more than 80% of the variance (**Figure 4B**). EM2 varies within the wide size range between 1.37 and 8.4 Φ, and the coarse end-member EM3 varies in the size range from −0.9 to 5.7 Φ. The proportions of the finest end-member EM1 vary in a large range from 20 to 100% (average ∼70%) (**Figure 3**), and the proportions of the EM2 vary from 0 to 80% (average ∼25%). The coarsest end-member EM3 varies between 0 and 51% with an average value of ∼5%. EM1 and EM2 display opposite patterns from the mid-Holocene to the present (**Figure 3**). The EM3 variation shows a generally similar trend compared with the mean grain size.

Geochemical Element Concentrations

The major and trace elements of Core K17 sediment are illustrated in **Figure 5**. Major elements include SiO_2 (48.9–82.1%), Al_2O_3 (3.7–15.4%), CaO (2.1–19.1%), K_2O (0.8–2.2%), Na_2O (0.5–1.6%), and TiO_2 (0.3–0.9%); trace elements are Rb (54.8–118.0 μg/g), Sr (116.4–726.4 μg/g), Cu (5.6–17.4 μg/g), and Pb (19.8–51.4 μg/g). The temporal patterns of Al_2O_3, K_2O, Na_2O, TiO_2, Rb, Pb, and Cu are basically similar in their distribution (**Figure 5**), having a drastic decrease of approximately 2900 and 3900 cal yr BP; SiO_2 displays almost the opposite character to those elements, and CaO and Sr have similar temporal distribution patterns, with an abrupt change of 2600 cal yr BP.

Sr-Nd Isotopic Compositions

The $^{87}Sr/^{86}Sr$ and εNd values of the silicate fraction of Core K17 are listed in **Table 3**. The $^{87}Sr/^{86}Sr$ ratios ranged from 0.72018 to 0.72636, and the εNd values varied from −10.28 to −7.06. The $^{87}Sr/^{86}Sr$ ratios exhibited a slight decreasing tendency, and the εNd values showed no significant variation during the studied timescale, except for one point (1–2 cm) of the core.

DISCUSSION

Provenance Discrimination

Sr-Nd isotopes are one of the widely used proxies to determine sediment provenance (Wei et al., 2012; Cao et al., 2015). However, the isotopic composition of marine sediments could be affected by authigenic, biogenic, and grain-size effects during the transport and deposition processes (Bayon et al., 2002; Dou et al., 2012; Hu et al., 2020) and, therefore, should be eliminated before using Sr-Nd isotopes to trace provenance.

Although the grain-size effect is very common for geochemical compositions (Wu et al., 2019), the $^{87}Sr/^{86}Sr$ ratios and εNd values are not significantly correlated with mean grain size (**Figure 6A**), indicating that the grain-size effect is negligible for Sr-Nd isotopes. Furthermore, there are no significant correlations between the $^{87}Sr/^{86}Sr$ and εNd values and the Fe_2O_3 values in this core sediment (**Figure 6B**), suggesting that authigenic Fe oxides or oxyhydroxides have little influence on isotopic composition. $^{87}Sr/^{86}Sr$ ratios are possibly controlled by the carbonate content, resulting from the isomorphic substitution between Ca in calcium carbonate and Sr from seawater (Hu et al., 2013). However, a very low correlation is observed between the $^{87}Sr/^{86}Sr$ ratios and CaO values (**Figure 6C**). Therefore, Sr-Nd isotopic compositions of these core sediments are considered reliable for tracing sediment provenances at the study site.

The potential sediment sources surrounding Core K17 include the Kelantan River and Pahang River in the Malay Peninsula, the

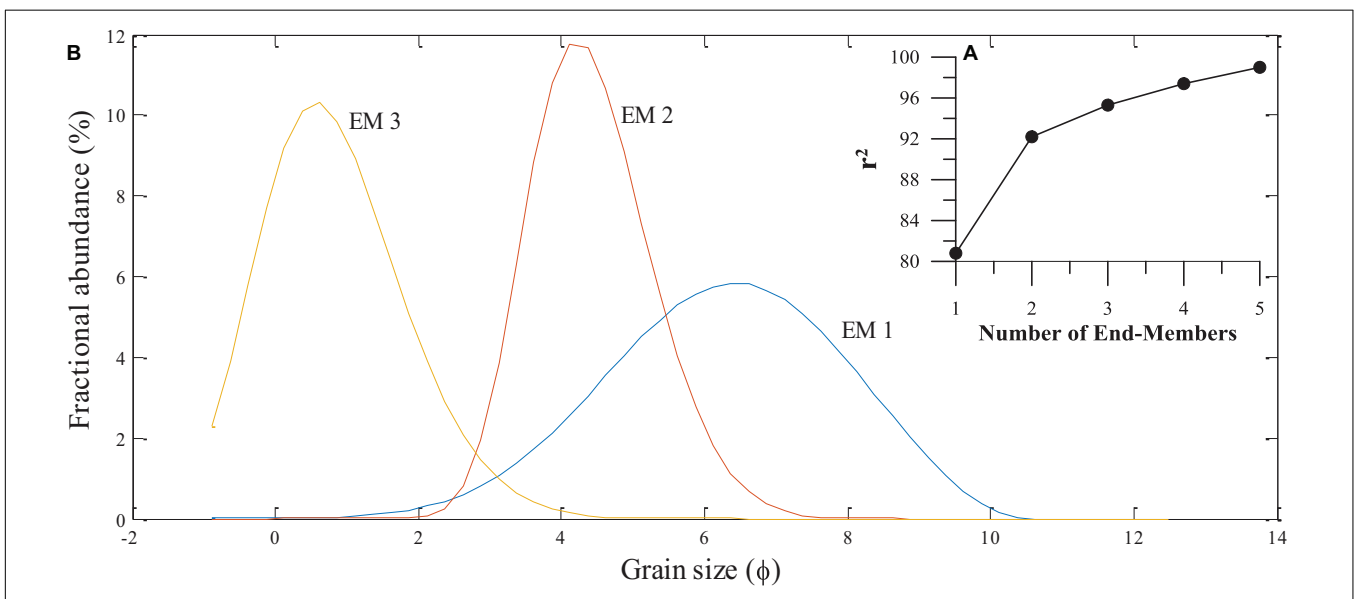

FIGURE 4 | (A) Fraction of data variance explained by the unmixing model vs. numbers of end-members. **(B)** Volume percent vs. grain-size (Φ) diagram of the three end-members (EM1, EM2, and EM3) identified in Core K17.

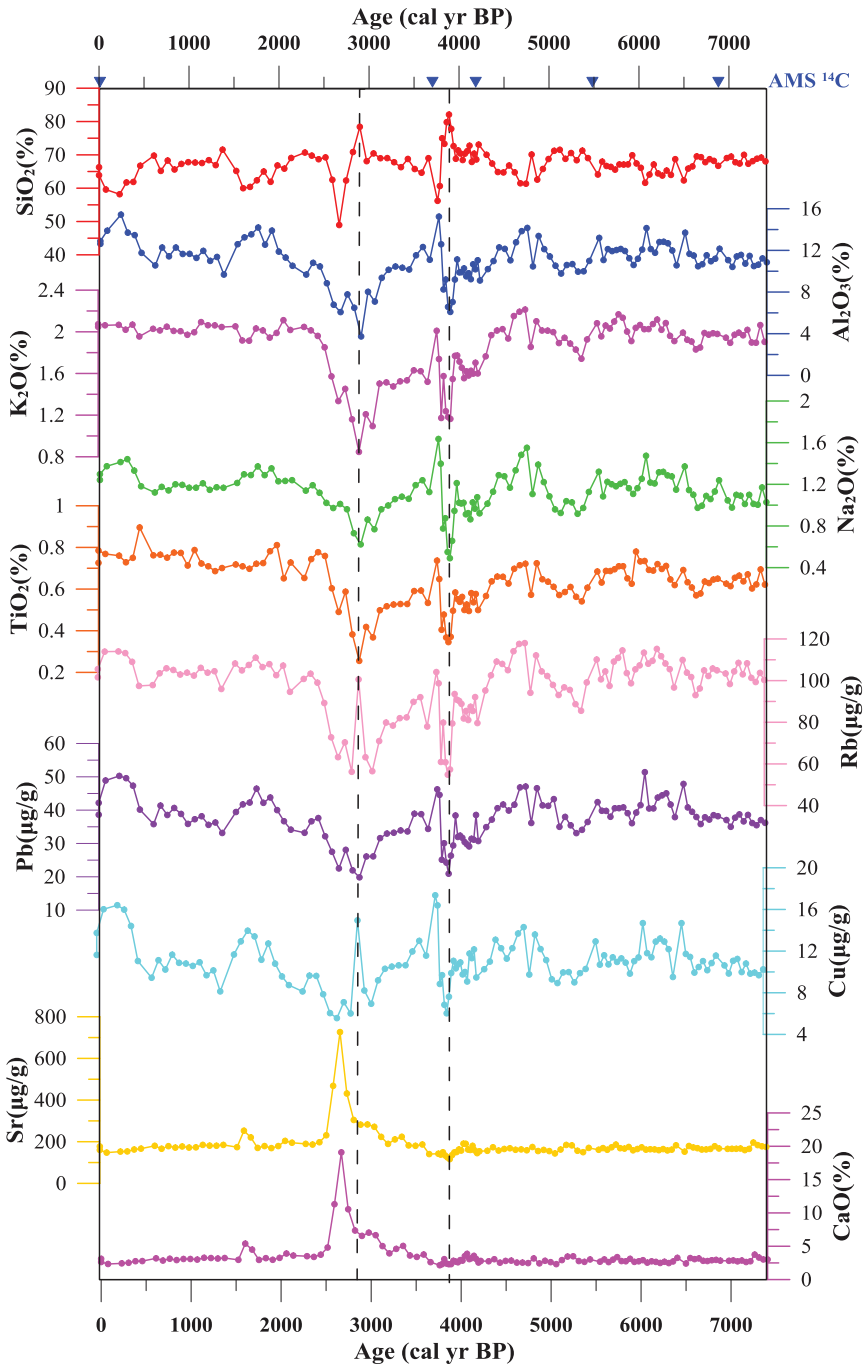

FIGURE 5 | Variations in major and trace elements of Core K17.

Mekong River in the Indochina Peninsula, the Chao Phraya River and other rivers in the Gulf of Thailand, and rivers in Borneo. The $^{87}Sr/^{86}Sr$ ratios are plotted against εNd values in Core K17 and potential provenances in the surrounding regions (**Figure 7**). Most of the εNd values and $^{87}Sr/^{86}Sr$ ratios of Core K17 are concentrated in the range of the Kelantan River, whereas the other three points fall in the field of the Mekong River, close to the range of the Kelantan River in **Figure 7**.

It seems that both the Kelantan River and Mekong River are the sediment sources of the Core K17. These three samples all fall in or close to the overlapping part of Kelantan River and Mekong River, which are 10–11, 20–21, and 30–31 cm sediment layers, respectively. The grain sizes of these three samples are coarser than the average grain size of other Sr-Nd sediment layers in this core. Sr-Nd values from other older samples all fall in the Kelantan River. Therefore, these three coarser samples may not

TABLE 3 | Sr and Nd isotopes of sediments in the Core K17 and potential river end members.

Sediment location	Depth (cm)	Age (cal yr BP)	$^{87}Sr/^{86}Sr$	$^{143}Nd/^{144}Nd$	ε Nd	Data sources
K17	1–2	0	0.72636	0.512276	−7.06	This study
K17	10–11	610	0.72066	0.512111	−10.28	This study
K17	30–31	2135	0.72056	0.512117	−10.16	This study
K17	40–41	2898	0.72018	0.512119	−10.12	This study
K17	50–51	3660	0.72151	0.512157	−9.38	This study
K17	70–71	4218	0.72150	0.512140	−9.71	This study
K17	80–81	4807	0.72150	0.512158	−9.36	This study
K17	100–101	5925	0.72093	0.512139	−9.73	This study
K17	120–121	6880	0.72101	0.512153	−9.46	This study
K17	130–131	7358	0.72196	0.512131	−9.89	This study
Kelantan River	Surface	_	0.72031	0.512132	−9.87	This study
Kelantan River	Surface	_	0.72307	0.512202	−8.51	This study
Kelantan River	Surface	_	0.72971	0.512225	−8.06	This study
Kelantan River	Surface	_	0.72721	0.512206	−8.43	This study
Kelantan River	Surface	_	0.72285	0.512285	−6.89	This study
Pahang River	Surface	_	0.74043	0.512130	−9.91	This study
Pahang River	Surface	_	0.74230	0.512128	−9.95	This study
Pahang River	Surface	_	0.73603	0.512141	−9.69	This study
Pahang River	Surface	_	0.74255	0.512156	−9.40	This study
Pahang River	Surface	_	0.74366	0.512136	−9.79	This study
Tha Chin River	Surface	_	0.720434	0.511878	−14.82	Wu et al., unpublished
Tha Chin River	Surface	_	0.734096	0.511903	−14.33	Wu et al., unpublished
Mae Klong River	Surface	_	0.753236	0.511820	−15.95	Wu et al., unpublished
Mae Klong River	Surface	_	0.743226	0.511840	−15.56	Wu et al., unpublished
Bang Pakong River	Surface	_	0.716848	0.512086	−10.77	Wu et al., unpublished
Bang Pakong River	Surface	_	0.719631	0.512132	−9.87	Wu et al., unpublished
Chao Phraya River	Surface	_	0.722863	0.512055	−11.36	Wu et al., unpublished
Chao Phraya River	Surface	_	0.718993	0.512067	−11.15	Wu et al., unpublished
Mekong River	Surface	_	0.720276	0.512131	−9.89	Liu et al., 2007
Mekong River	Surface	_	0.720699	0.512115	−10.2	Liu et al., 2007
Mekong River	Surface	_	0.721307	0.512082	−10.85	Liu et al., 2007
Mekong River	Surface	_	0.722173	0.512104	−10.42	Liu et al., 2007
Mekong River	Surface	_	0.721801	0.512098	−10.53	Liu et al., 2007
Offshore Borneo	Surface	_	0.717031	0.512216	−8.23	Wei et al., 2012
Offshore Borneo	Surface	_	0.709882	0.512282	−6.95	Wei et al., 2012
Offshore Borneo	Surface	_	0.715360	0.512200	−8.54	Wei et al., 2012
Offshore Borneo	Surface	_	0.720602	0.512189	−8.76	Wei et al., 2012
Offshore Borneo	Surface	_	0.719912	0.512191	−8.72	Wei et al., 2012

eNd = 10,000 × ($^{143}Nd/^{144}Nd$/0.512638−1).

be transported from the Mekong River. In fact, the Core K17 is close to the Kelantan estuary; approximately 13.9 Mt/year of sediment from the Kelantan River is discharged into the SCS (Liu et al., 2016), most of which is deposited in the estuary, with the remainder transported to the western Sunda Shelf (Koopmans, 1972; Wang et al., 2020). Our recent work used geochemical and mineral evidence to reveal that fine-grained modern sediment from the Kelantan River can be transported to the central Sunda Shelf (Wu et al., 2020). Although the Mekong River delivers approximately 160 Mt/year to the SCS, approximately 80% of the Mekong-delivered sediment is trapped within the delta area (Xue et al., 2010). Large amounts of Mekong River sediments are deposited near the Mekong River mouth in summer, and only a small fraction of these sediments are re-suspended and dispersed toward the southwest into the Gulf of Thailand during the northeast monsoon (Xue et al., 2012). During the last glacial period with a low relative sea level, sediments from the Mekong River were directly input into the southern SCS by the paleo-Mekong River and not discharged into the Sundaland (Jiwarungrueangkul et al., 2019b). Additionally, the distribution of clay mineral assemblages in the surface sediments of the SCS indicates that most of the kaolinite, accounting for more than 50% of clay minerals offshore of Malaysia, is from the Malay Peninsula and not the Mekong River (Liu et al., 2016). Therefore, we suggest that the Kelantan River is the primary provenance of Core K17.

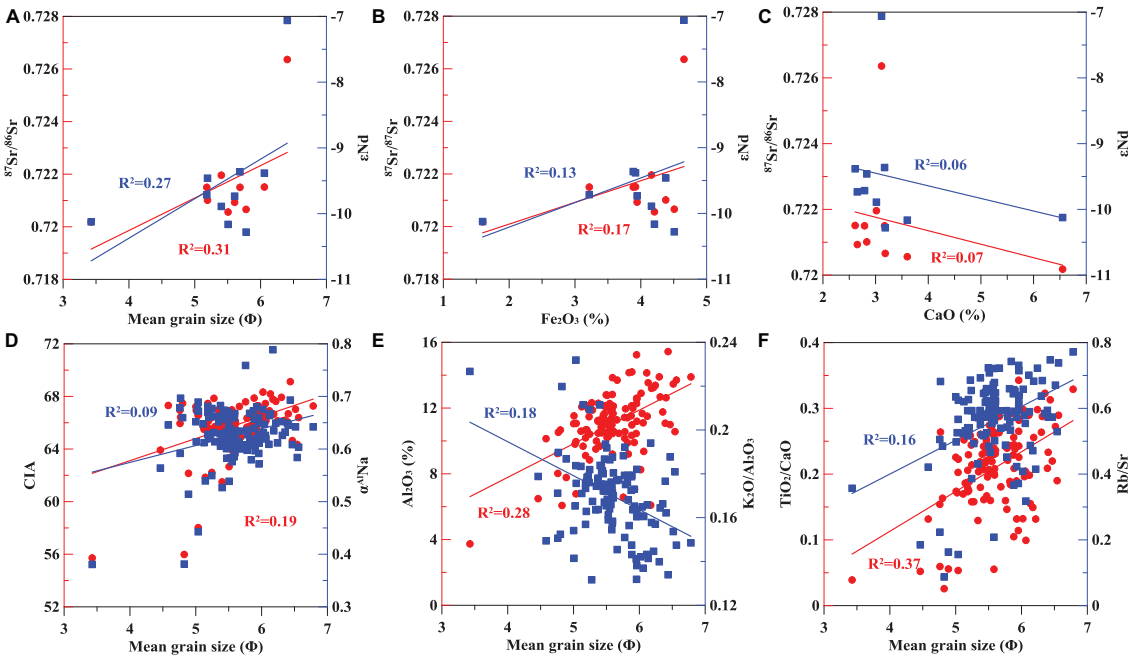

FIGURE 6 | Correlation analysis of Sr-Nd isotopic compositions, mean grain size, Fe_2O_3, MnO, and CaO concentrations, and weathering and terrigenous input indicators in Core K17. **(A–C)** Correlations between Sr-Nd isotopic compositions and mean grain size, Fe_2O_3 and CaO concentrations in core K17, respectively. **(D–F)** Correlations between mean grain size and chemical weathering indicators (CIA, $a^{Al}Na$ and K_2O/Al_2O_3), and terrigenous input indicators (TiO_2/CaO and Rb/Sr ratios) in core K17, respectively.

Sedimentary Responses to Climate Changes and Human Activities Over the Past 7400 cal yr BP

Weathering and Terrigenous Input Indicators

Chemical weathering is an important process for modifying the mineral and chemical compositions of terrigenous sediments (Hu et al., 2020). The degree of chemical weathering under specific environmental conditions is primarily controlled by climate (White and Blum, 1995). Generally, high temperatures and heavy precipitation favor more intense chemical weathering, whereas low temperatures and less precipitation hinder the reactions involved in chemical weathering (White and Blum, 1995; Huang et al., 2018). Here, the chemical index of alteration (CIA), $\alpha^{Al}Na$, and the K_2O/Al_2O_3 ratio were used to estimate chemical weathering intensity and variation. The CIA [defined as CIA = $Al_2O_3/(Al_2O_3 + CaO^* + Na_2O + K_2O) \times 100$, molar proportions; CaO^* refers to the CaO content of the silicate fraction] and $\alpha^{Al}Na$ [defined as $\alpha^{Al}Na = (Al/Na)_{sediment}/(Al/Na)_{UCC}$, molar proportions] are widely used to estimate the chemical weathering intensity recorded in sediments (Nesbitt and Young, 1982; Garzanti et al., 2013; Liu et al., 2020). Higher CIA and $\alpha^{Al}E$ values correspond to stronger chemical weathering intensity. CaO^* in CIA is corrected by comparing the molar contents of CaO with Na_2O, and the lower value is regarded as the CaO content in the silicate fraction (Singh et al., 2005; Liu et al., 2020). K_2O is preferentially leached in aqueous fluids compared to the immobile Al_2O_3 during the chemical weathering process (Nesbitt and Young, 1982); therefore, a lower K_2O/Al_2O_3 ratio could indicate increased chemical weathering related to strengthened monsoon rainfall, according to the basic principles of silicate weathering (Wei et al., 2004; Clift et al., 2014; Jiwarungrueangkul et al., 2019a).

TiO_2/CaO and Rb/Sr ratios were used to evaluate the variation of terrigenous sediment input related to erosion in this study (Jiwarungrueangkul et al., 2019b; Li et al., 2019). The Ti content in terrigenous sediments is stable in hypergenesis, and the Ti in marine sediments is widely believed to be primarily derived from the input of terrestrial clastic materials (Chen et al., 2013; Li et al., 2019). CaO in marine sediment primarily originates from biogenic input; thus, the TiO_2/CaO ratio can reflect the relative magnitudes of terrigenous clastics and biogenic inputs (Clift et al., 2014; Cao et al., 2015). Rb and Sr are primarily distributed in minerals bearing K (e.g., mica and K-feldspar) and Ca (e.g., carbonate), respectively; thus, Rb/Sr ratio can be used as another indicator of terrigenous sediment input (Li et al., 2019). Higher TiO_2/CaO and Rb/Sr ratios reflect enhanced terrigenous input to the core.

In previous studies, the finest end member was usually interpreted as fluvial/terrigenous input (Stuut and Lamy, 2004; Wan et al., 2007). Due to the dominant fraction of EM1 in the three end members and the overwhelming terrigenous element concentrations (e.g., SiO_2 and Al_2O_3; **Figure 3**) of sediments in Core K17, the finest end-member EM1 was interpreted as fluvial terrigenous sediment input from the Kelantan River in this study.

To ensure that chemical weathering and terrigenous input indicators are reliable for use in the study region, other factors,

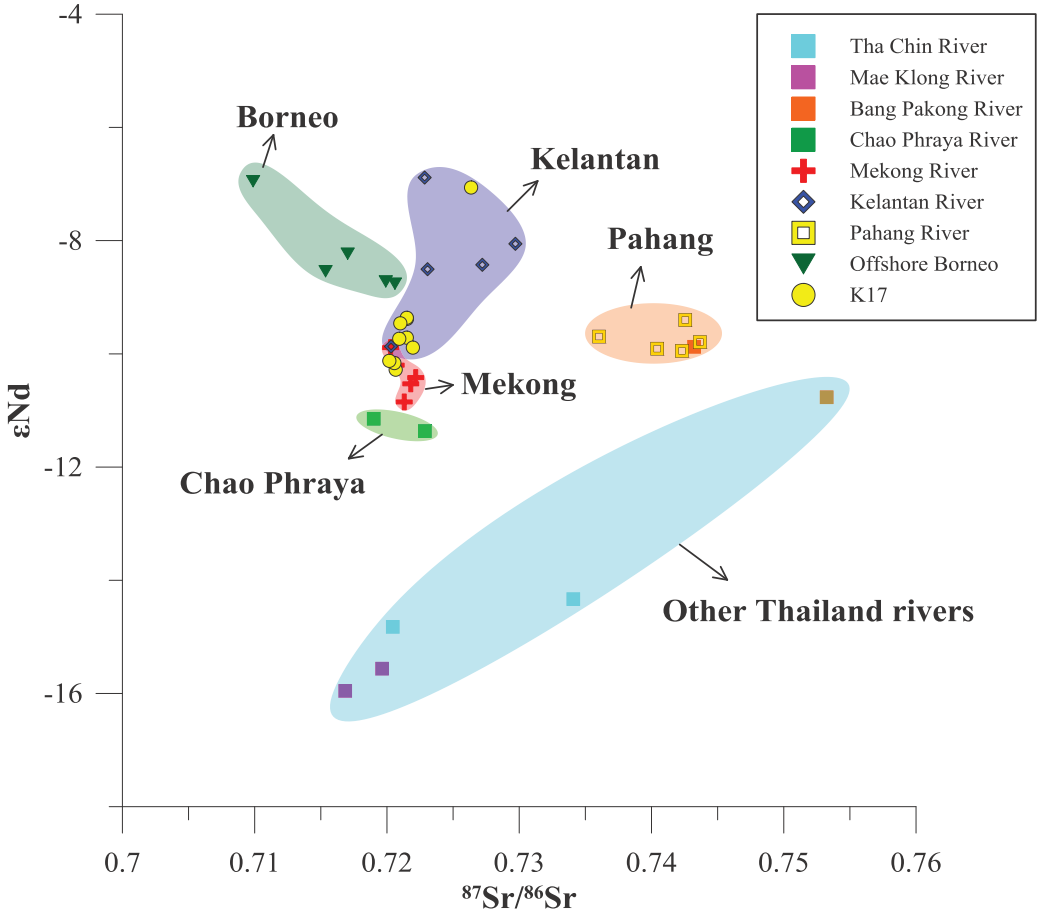

FIGURE 7 | The $^{87}Sr/^{86}Sr$ ratios versus εNd values plot for the Core K17, with sediments of Mekong River (Liu et al., 2007), Borneo offshore (Wei et al., 2012), Chao Phraya River and other Thailand rivers (Wu et al., unpublished), and Pahang and Kelantan River (this study).

including provenance changes, sea-level change, and hydraulic sorting by oceanic currents need to be considered (Hu et al., 2020). Because of the relatively constant source of Core K17 (**Figure 7**), provenance changes could not significantly influence weathering and terrigenous indicators. Sea level change played an important role in controlling terrigenous sediment input to the southern SCS before or during the early Holocene (Jiwarungrueangkul et al., 2019a) but is relatively constant with a weak fluctuation since ca. 7–8 ka on the Sunda Shelf, when the coastline reached a modern position (Steinke et al., 2003; Hanebuth et al., 2011). Thus, the influence of sea level changes is negligible. There were no significant correlations between the mean grain size and weathering and erosion indicators (i.e., CIA, K_2O/Al_2O_3, $\alpha^{Al}Na$, TiO_2/CaO, and Rb/Sr; **Figures 6D–F**), suggesting that these indicators are not influenced by transport processes or hydraulic sorting.

Climatic and Anthropogenic Impacts on the Weathering and Terrigenous Input Processes Over the Past 7400 cal yr BP

Monsoon rainfall intensity and temperature variations in the study area could lead to typical changes in chemical weathering and erosion over time (Huang et al., 2018; Li et al., 2019). Based on temporal variations in weathering and terrigenous input related to erosion processes (**Figure 8**), we suggest a four-stage sedimentary evolution in Core K17 over the last 7400 cal yr BP.

The first stage corresponds to a period of 7400–3700 cal yr BP. Stable CIA, $\alpha^{Al}Na$, and K_2O/Al_2O_3 values indicate stable chemical weathering during this period (**Figures 8C–E**). The relatively stable TiO_2/CaO and Rb/Sr ratios during this interval suggest relatively stable terrigenous sediment input (**Figures 8G,H**). Furthermore, EM1 displays a relatively stable pattern but contains fluctuations that indicate constant Kelantan River discharge due to stable chemical weathering and terrigenous input (**Figure 8F**). The monsoon precipitation from the $\delta^{18}O$ record gradually increased from 7400 to ca. 5000 cal yr BP and remained stable with heavy rainfall during 5000–3700 cal yr BP (Partin et al., 2007; Carolin et al., 2016; **Figure 8A**), contributing to more intense chemical weathering and terrigenous sediment input from the Kelantan River drainage. However, the temperature gradually decreased during this interval (**Figure 8B**), apparently reducing weathering and sediment input. Therefore, the relatively stable chemical weathering and terrigenous sediment input were probably

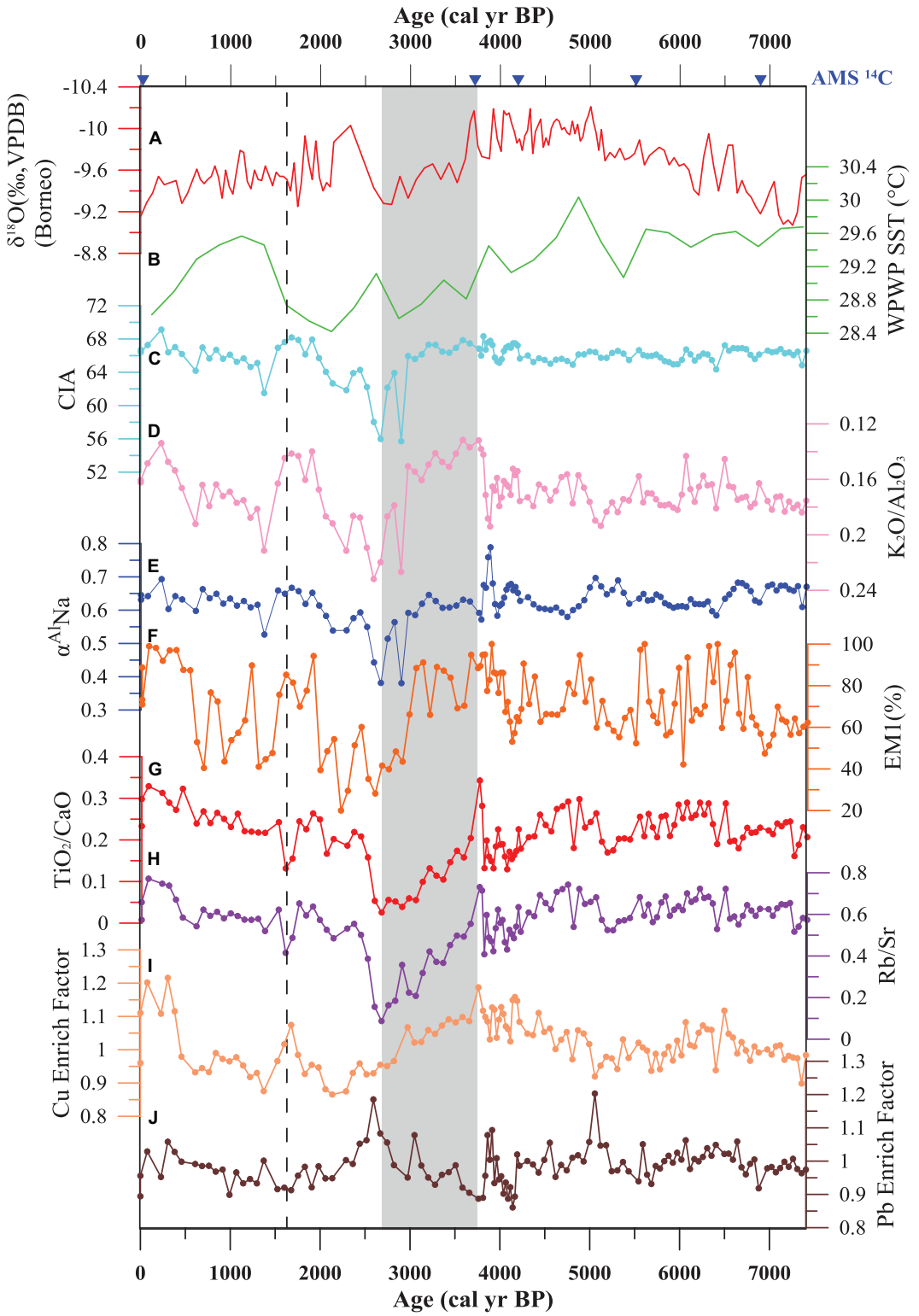

FIGURE 8 | Comparison of the Core K17 records with other representative paleoclimate records since 7400 cal yr BP: **(A)** Rainfall patterns from Borneo cave stalagmite $\delta^{18}O$ (Partin et al., 2007); **(B)** sea surface temperature (SST) of the Western Pacific Warm Pool (WPWP; Stott et al., 2004); **(C)** CIA from Core K17; **(D)** K_2O_3/Al_2O_3 from Core K17; **(E)** αAlNa from Core K17; **(F)** EM1 volume from Core K17; **(G)** TiO_2/CaO from Core K17; **(H)** Rb/Sr from Core K17; **(I)** Cu enrichment factor from Core K17; and **(J)** Pb enrichment factor from Core K17. The shadow area represents the interval of the second stage. The dotted line represents the boundary of third stage and fourth stage.

balanced by increasing rainfall and decreasing temperatures during this period.

The second stage ranged from 3700 to 2700 cal yr BP. Decreasing CIA, $\alpha^{Al}Na$, and K_2O/Al_2O_3 values suggest weaker chemical weathering and less sediment production in this interval. Less terrigenous sediment input is indicated by decreasing TiO_2/CaO and Rb/Sr ratios. Less monsoon rainfall and decreasing temperature led to weaker chemical weathering and less sediment transport to the western Sunda Shelf during this period (Stott et al., 2004; Partin et al., 2007). Due to weaker chemical weathering, fine EM1 also displayed a decreasing trend, corresponding to less Kelantan River discharge to the western Sunda Shelf during this interval. Additionally, weaker chemical weathering and less precipitation in this period were reported in the Pearl River estuary (Hu et al., 2013; Huang et al., 2018) and the Red River estuary (Wan et al., 2015) in the northern SCS, probably indicating the synchronous variations of climate change during this period in the SCS.

The third stage spanned 2700–1600 cal yr BP. Increasing CIA, $\alpha^{Al}Na$, and K_2O/Al_2O_3 values suggest stronger chemical weathering in this interval, and TiO_2/CaO and Rb/Sr ratios show an increasing trend, indicating more terrigenous sediment input. Heavy rainfall during this period possibly played a more important role than lower temperature and resulted in more intense chemical weathering and terrigenous sediment input. Therefore, EM1 also showed an increasing pattern similar to chemical weathering, indicating increasing river input.

The fourth stage corresponds to the interval since 1600 cal yr BP. Increasing CIA, $\alpha^{Al}Na$, and K_2O/Al_2O_3 values indicate stronger chemical weathering, which contributed to the production of more terrigenous sediment from the Kelantan River; decreasing monsoon precipitation from $\delta^{18}O$ records (Partin et al., 2007; Carolin et al., 2016) hindered river sediment production and transportation into the western Sunda Shelf in this period. Increasing TiO_2/CaO and Rb/Sr ratios suggest increasing terrigenous sediment input. EM1 also indicates increasing river discharge with fluctuations corresponding to stronger chemical weathering and increasing rainfall. Less precipitation and falling temperature with increasing weathering and erosion suggest no direct relationship between weathering and erosion and precipitation and temperature in this interval. Thus, climate change cannot be solely responsible for weathering/erosion changes since 1600 cal yr BP. A similar decoupling relationship between climate and weathering/erosion was reported in the Pearl River estuary (Huang et al., 2018) and the Red River estuary (Wan et al., 2015) in the northern SCS. We suggest that human activities have dominated chemical weathering and terrigenous input relative to climate change since 1600 cal yr BP. The Malay-Thai Peninsula contains many archeological sites from 6000 to 600 cal yr BP and had become a primary region of settlement in the early historic period during 2000–1400 cal yr BP (Horton et al., 2005), indicating that human society in the Malay Peninsula formed at least as early as 2000 cal yr BP. Since ca. 2000 cal yr BP, rice cultivation has been common in Southeast Asia (Liang et al., 2011). During 2000–1000 cal yr BP, both sides of the Malay Peninsula were important centers of East–West trade, and small-scale agricultural centers were established in some river basins (Liang et al., 2011). Agricultural development caused partial soil erosion, corresponding to the general increase in chemical weathering and terrigenous input (CIA, $\alpha^{Al}Na$, K_2O/Al_2O_3, TiO_2/CaO, Rb/Sr, and EM1) in Core K17 during this period (**Figure 8**).

Enrichment factor (EF) is widely used to discriminate natural and anthropogenic sources and to elevate environmental contamination (Wan et al., 2015). EF is calculated using the following equation: $EF = (X_{sample}/Al_{sample})/(X_{baseline}/Al_{baseline})$, where X_{sample} ($X_{baseline}$) and Al_{sample} ($Al_{baseline}$) are heavy metal concentrations and aluminum contents of samples (background references), and average elements concentration of samples below 84 cm depth (older than 5000 cal yr B P.) is chosen as the baseline, which is regarded as not influenced by anthropogenic process. Our results show that the EF values of Cu and Pb increased dramatically after 1600 cal yr BP (**Figures 8I,J**), which is closely related to mining and metalworking activities due to increasing requirements of tools for agriculture, corresponding to an increasing impact of human activities. There is a long history of tin and gold mining in Peninsular Malaysia at least before the 9th century (Balamurugan, 1991), related metal elements such as Cu and Pb are very common in tin or gold deposits. Burning of trees to smelt metals in the ancient could strengthen weathering and erosion since 1600 cal yr BP. Furthermore, the enrichment of Cu and Pb seems to be related to the disposal of sewage effluent, indicating an increase in human activity (Hu et al., 2013, 2020; Huang et al., 2018). Relatively higher enrichment of Cu and Pb were also observed in some sediment sequences before 1600 cal yr BP (**Figures 8I,J**), perhaps reflecting fluvial erosion related to harsh weather conditions during this period (Hu et al., 2020), such as flooding, which occurs frequently in the Kelantan River basin (Koopmans, 1972). However, more research is needed to clarify these mechanisms. The initial time at which human activity overwhelmed natural processes in our study is similar to that in the Pearl River Delta (2000 cal yr BP) (Huang et al., 2018), the Red River drainage (1800 cal yr BP) (Wan et al., 2015), and Taiwan (1500 cal yr BP) (Hu et al., 2020). Therefore, since 1600 cal yr BP, increased human activity has been the dominant influence on the natural landscape of Kelantan River drainage by agriculture and related mining activities. Compared the established variations in erosion and weathering rates from Sunda Shelf with other studies from the Southeast Asia, especially in the northern SCS (Wan et al., 2015; Huang et al., 2018), our results show a similar variation trend with them, but the accurate changing periods between these studies have some differences. It is worth noting that, after about 2000 cal yr BP, they all display a remarkable increasing trend. Therefore, we believe the Southeast Asia have similar variations trend in erosion and weathering rates, and human activities overwhelming the nature in erosion and weathering share a similar period in the Southeast Asia.

CONCLUSION

Provenance analysis from Sr-Nd isotopic evidence for Core K17 in the western Sunda Shelf suggests that the Kelantan

River is the major sediment contributor. The sediment succession of Core K17 can be divided into four stages according to chemical weathering and terrigenous input indicators. During stage 1 (7400–3700 cal yr BP), increasing precipitation and decreasing temperature jointly controlled relatively stable chemical weathering and terrigenous sediment input. Dramatically decreasing weathering and terrigenous input during stage 2 (3700–2700 cal yr BP) coincides well with less precipitation and lower temperature, resulting in weaker weathering and erosion. The period of 2700–1600 cal yr BP corresponds to the third stage, in which heavy rainfall played a more important role than low temperature in controlling weathering and erosion and led to increasing terrigenous input. For the late Holocene (stage 4, since 1600 cal yr BP), weathering and sediment inputs in the study core have likely been dominantly influenced by human activities due to decoupling between weathering/erosion and climate change and increasing agriculture and mining activities.

DATA AVAILABILITY STATEMENT

The raw data supporting the conclusions of this article will be made available by the authors, without undue reservation.

AUTHOR CONTRIBUTIONS

KW interpreted the data and wrote the manuscript. XS conceived and designed the project. KW and BW recovered the sediment core. KW and HZ did the experiments about the grain size, geochemistry, and isotopes. PC and CR collected the samples in the field. ZL, BW, and JL revised the manuscript. All authors contributed to the article and approved the submitted version.

FUNDING

This work was supported by the National Program on Global Change and Air-Sea Interaction (GASI-GEOGE-03 and GASI-02-SCS-CJB01), the Natural Science Foundation of China-Shandong Joint Fund for Marine Science Research Centers (U1606401), the Scientific and Technological Innovation Project Financially supported by Qingdao National Laboratory for Marine Science and Technology (2015ASKJ03), the China–Malaysia cooperation project "Effect on variability of seasonal monsoon on sedimentary process in Peninsular Malaysia waters," and the Taishan Scholar Program of Shandong.

ACKNOWLEDGMENTS

We thank staff of National University of Malaysia, crew of "R.V. DISCOVERY," and Xisheng Fang, Xin Shan, Haitao Zhang, and Taoyu Xu from the First Institute of Oceanography, Ministry of Natural Resources for sample collection on board, and Xingquan Sun and Wenxing Ye from the Ocean University of China for sample pretreatment.

REFERENCES

Awadalla, S., and Noor, I. M. (1991). Induced climate change on surface runoff in Kelantan Malaysia. *Int. J. Water Resour. Dev.* 7, 53–59. doi: 10.1080/07900629108722492

Balamurugan, G. (1991). Tin mining and sediment supply in Peninsular Malaysia with special reference to the Kelang River basin. *Environmentalist* 11, 281–291. doi: 10.1007/BF01266561

Bayon, G., German, C. R., Boella, R. M., Milton, J. A., Taylor, R. N., and Nesbitt, R. W. (2002). An improved method for extracting marine sediment fractions and its application to sr and nd isotopic analysis. *Chem. Geol.* 187, 179–199. doi: 10.1016/S0009-2541(01)00416-8

Bi, L., Yang, S., Li, C., Guo, Y., Wang, Q., Liu, J. T., et al. (2015). Geochemistry of river-borne clays entering the east china sea indicates two contrasting types of weathering and sediment transport processes. *Geochem. Geophys. Geosyst.* 16, 3034–3052. doi: 10.1002/2015GC005867

Cao, P., Shi, X., Li, W., Liu, S., Yao, Z., Hu, L., et al. (2015). Sedimentary responses to the Indian Summer Monsoon variations recorded in the southeastern Andaman Sea slope since 26 ka. *J Asian Earth Sci.* 114, 512–525. doi: 10.1016/j.jseaes.2015.06.028

Carolin, S. A., Cobb, K. M., Lynch-Stieglitz, J., Moerman, J. W., Partin, J. W., Lejau, S., et al. (2016). Northern Borneo stalagmite records reveal West Pacific hydroclimate across MIS 5 and 6. *Earth Planet. Sci. Lett.* 439, 182–193. doi: 10.1016/j.epsl.2016.01.028

Chen, H. F., Yeh, P. Y., Song, S. R., Hsu, S. C., Yang, T. N., Wang, Y., et al. (2013). The Ti/Al molar ratio as a new proxy for tracing sediment transportation processes and its application in Aeolian events and sea level change in East Asia. *J. Asian Earth Sci.* 73, 31–38. doi: 10.1016/j.jseaes.2013.04.017

Clift, P. D., Wan, S., and Blusztajn, J. (2014). Reconstructing chemical weathering, physical erosion and monsoon intensity since 25 Ma in the northern South China Sea: a review of competing proxies. *Earth Sci. Rev.* 130, 86–102. doi: 10.1016/j.earscirev.2014.01.002

Corella, J. P., Stefanova, V., El Anjoumi, A., Rico, E., Giralt, S., Moreno, A., et al. (2013). A 2500-year multi-proxy reconstruction of climate change and human activities in northern Spain: the Lake Arreo record. *Palaeogeogr. Palaeoclimatol. Palaeoecol.* 386, 555–568. doi: 10.1016/j.palaeo.2013.06.022

Dou, Y., Yang, S., Liu, Z., Shi, X., Li, J., Yu, H., et al. (2012). Sr–Nd isotopic constraints on terrigenous sediment provenances and Kuroshio Current variability in the Okinawa Trough during the late Quaternary. *Palaeogeogr. Palaeoclimatol. Palaeoecol.* 365–366:38–47. doi: 10.1016/j.palaeo.2012.09.003

Folk, R. L., Andrews, P. B., and Lewis, D. W. (1970). Detrital sedimentary rock classification and nomenclature for use in New Zealand. *N. Z. J. Geol. Geophys.* 13, 937–968. doi: 10.1080/00288306.1970.10418211

Garzanti, E., Limonta, M., Resentini, A., Bandopadhyay, P. C., Najman, Y., Andò, S., et al. (2013). Sediment recycling at convergent plate margins (Indo-Burman Ranges and Andaman–Nicobar Ridge). *Earth Sci. Rev.* 123, 113–132. doi: 10.1016/j.earscirev.2013.04.008

Hanebuth, T. J. J., Stattegger, K., and Grootes, P. M. (2000). Rapid flooding of the Sunda shelf: a late-glacial sea-level record. *Science* 288, 1033–1035. doi: 10.1126/science.288.5468.1033

Hanebuth, T. J. J., Voris, H. K., Yokoyama, Y., Saito, Y., and Okuno, J. (2011). Formation and fate of sedimentary depocentres on Southeast Asia's Sunda Shelf over the past sea-level cycle and biogeographic implications. *Earth Sci. Rev.* 104, 92–110. doi: 10.1016/j.earscirev.2010.09.006

Horton, B. P., Gibbard, P. L., Mine, G. M., Morley, R. J., Purintavaragul, C., and Stargardt, J. M. (2005). Holocene sea levels and palaeoenvironments, Malay-Thai Peninsula, southeast Asia. *Holocene* 15, 1199–1213.

Hu, D., Clift, P. D., Böning, P., Hannigan, R., Hillier, S., Blusztajn, J., et al. (2013). Holocene evolution in weathering and erosion patterns in the Pearl River delta. *Geochem. Geophys. Geosyst.* 14, 2349–2368. doi: 10.1002/ggge.20166

Hu, S., Zeng, Z., Fang, X., Yin, X., Chen, Z., Li, X., et al. (2020). Increasing terrigenous sediment supply from Taiwan to the southern Okinawa Trough over the last 3000 years evidenced by Sr-Nd isotopes and geochemistry. *Sediment. Geol.* 406, 105725. doi: 10.1016/j.sedgeo.2020.105725

Huang, C., Zeng, T., Ye, F., Xie, L., Wang, Z., Wei, G., et al. (2018). Natural and anthropogenic impacts on environmental changes over the past 7500 years based on the multi-proxy study of shelf sediments in the northern South China Sea. *Quat. Sci. Rev.* 197, 35–48. doi: 10.1016/j.quascirev.2018.08.005

Hutchison, C. S. (1968). Dating tectonism in the Indosinian-Thai-Malayan orogen by thermoluminescence. *Geol. Soc. Am. Bull.* 79, 375–386.

Jiwarungrueangkul, T., Liu, Z., Stattegger, K., and Sang, P. (2019a). Reconstructing chemical weathering intensity in the Mekong River basin since the Last Glacial Maximum. *Paleoceanogr. Paleoclimatol.* 34, 1710–1725. doi: 10.1029/2019PA003608

Jiwarungrueangkul, T., Liu, Z., and Zhao, Y. (2019b). Terrigenous sediment input responding to sea level change and East Asian monsoon evolution since the last deglaciation in the southern South China Sea. *Glob. Planet. Change* 174, 127–137. doi: 10.1016/j.gloplacha.2019.01.011

Joussain, R., Colin, C., Liu, Z., Meynadier, L., Fournier, L., Fauquembergue, K., et al. (2016). Climatic control of sediment transport from the Himalayas to the proximal NE Bengal Fan during the last glacial-interglacial cycle. *Quat. Sci. Rev.* 148, 1–16. doi: 10.1016/j.quascirev.2016.06.016

Kamarudin, M. K. A., Toriman, M. E., Rosli, M. H., Juahir, H., Aziz, N. A. A., Azid, A., et al. (2015). Analysis of meander evolution studies on effect from land use and climate change at the upstream reach of the Pahang River, Malaysia. *Mitig. Adapt. Strateg. Glob. Change* 20, 1319–1334. doi: 10.1007/s11027-014-9547-6

Koopmans, B. N. (1972). Sedimentation in the Kelantan Delta (Malaysia). *Sediment. Geol.* 7, 65–84. doi: 10.1016/0037-0738(72)90054-1

Li, J., Liu, S., Shi, X., Zhang, H., Fang, X., Cao, P., et al. (2019). Sedimentary responses to the sea level and Indian summer monsoon changes in the central Bay of Bengal since 40 ka. *Mar. Geol.* 415:105947. doi: 10.1016/j.margeo.2019.05.006

Li, J., Liu, S., Shi, X., Zhang, H., Fang, X., Chen, M., et al. (2018). Clay minerals and Sr-Nd isotopic composition of the Bay of Bengal sediments: implications for sediment provenance and climate control since 40 ka. *Quat. Int.* 493, 50–58. doi: 10.1016/j.quaint.2018.06.044

Liang, Z., Li, M., and Yang, B. (2011). *A History of Ancient Southeast Asia*. (Beijing: Peking University Press), 254–258.

Liu, S., Li, J., Zhang, H., Cao, P., Mi, B., Khokiattiwongc, S., et al. (2020). Complex response of weathering intensity registered in the Andaman Sea sediments to the Indian Summer Monsoon over the last 40 kyr. *Mar. Geol.* 426:106206. doi: 10.1016/j.margeo.2020.106206

Liu, Z., Colin, C., Huang, W., Le, K., Tong, S., Chen, Z., et al. (2007). Climatic and tectonic controls on weathering in South China and the Indochina Peninsula: clay mineralogical and geochemical investigations from the Pearl, Red, and Mekong drainage basins. *Geochem. Geophys. Geosyst.* 8:Q05005. doi: 10.1029/2006GC001490

Liu, Z., Wang, H., Hantoro, W., Sathiamurthy, E., Colin, C., Zhao, Y., et al. (2012). Climatic and tectonic controls on chemical weathering in tropical Southeast Asia (Malay Peninsula, Borneo, and Sumatra). *Chem. Geol.* 291, 1–12. doi: 10.1016/j.chemgeo.2011.11.015

Liu, Z., Zhao, Y., Colin, C., Stattegger, K., Wiesner, M. G., Huh, C. A., et al. (2016). Source-to-sink transport processes of fluvial sediments in the South China Sea. *Earth Sci. Rev.* 153, 238–273. doi: 10.1016/j.earscirev.2015.08.005

McLennan, S. M. (1993). Weathering and global denudation. *J. Geol.* 101, 295–303. doi: 10.1086/648222

Milliman, J. D., Farnsworth, K. L., and Albertin, C. S. (1999). Flux and fate of fluvial sediments leaving large islands in the East Indies. *J. Sea Res.* 41, 97–107. doi: 10.1016/S1385-1101(98)00040-9

Nesbitt, H. W., and Young, G. M. (1982). Early Proterozoic climates and plate motions inferred from major element chemistry of lutites. *Nature* 299, 715–717. doi: 10.1038/299715a0

Partin, J. W., Cobb, K. M., Adkins, J. F., Clark, B., and Fernandez, D. P. (2007). Millennial-scale trends in west Pacific warm pool hydrology since the Last Glacial Maximum. *Nature* 449, 452–455. doi: 10.1038/nature06164

Pelejero, C., Kienast, M., Wang, L., and Grimalt, J. O. (1999). The flooding of Sundaland during the last deglaciation: imprints in hemipelagic sediments from the southern South China Sea. *Earth Planet. Sci. Lett.* 171, 661–671. doi: 10.1016/S0012-821X(99)00178-8

Raj, J. K., Yusoff, I., and Abdullah, W. H. (2007). Past, present and future coastal changes at the Kuala Kemasin estuary, Kelantan State. *Bull. Geol. Soc. Malaysia* 53, 75–80. doi: 10.7186/bgsm53200712

Raymo, M. E., and Ruddiman, W. F. (1992). Tectonic forcing of late Cenozoic climate. *Nature* 359, 117–122. doi: 10.1038/359117a0

Reimer, P. J., Bard, E., Bayliss, A., Beck, J. W., Blackwell, P. G., Ramsey, C. B., et al. (2013). Selection and treatment of data for radiocarbon calibration: an update to the international calibration (IntCal) criteria. *Radiocarbon* 55, 1923–1945. doi: 10.1017/S003382220004889X

Singh, M., Sharma, M., and Tobschall, H. J. (2005). Weathering of the Ganga alluvial plain, northern India: implications from fluvial geochemistry of the Gomati River. *Appl. Geochem.* 20, 1–21. doi: 10.1016/j.apgeochem.2004.07.005

Southon, J., Kashgarian, M., Fontugne, M., Metivier, B., and Yim, W. W. (2002). Marine reservoir corrections for the Indian Ocean and Southeast Asia. *Radiocarbon* 44, 167–180. doi: 10.1017/S0033822200064778

Steinke, S., Kienast, M., and Hanebuth, T. J. J. (2003). On the significance of sea-level variations and shelf paleo-morphology in governing sedimentation in the southern South China Sea during the last deglaciation. *Mar. Geol.* 201, 179–206. doi: 10.1016/S0025-3227(03)00216-0

Stott, L., Cannariato, K., Thunell, R., Haug, G. H., Koutavas, A., and Lund, S. (2004). Decline of surface temperature and salinity in the western tropical Pacific Ocean in the Holocene epoch. *Nature* 431, 56–59. doi: 10.1038/nature02903

Stuut, J. B. W., and Lamy, F. (2004). Climate variability at the southern boundaries of the Namib (southwestern Africa) and Atacama (northern Chile) coastal deserts during the last 120,000 yr. *Quat. Res.* 62, 301–309. doi: 10.1016/j.yqres.2004.08.001

Tan, L., Shen, C., Löwemark, L., Chawchai, S., Edwards, R. L., Cai, Y., et al. (2019). Rainfall variations in central Indo-Pacific over the past 2,700 y. *Proc. Natl. Acad. Sci. U.S.A.* 116, 17201–17206. doi: 10.1073/pnas.1903167116

Tangang, F. T., Xia, C., Qiao, F., Juneng, L., and Shan, F. (2011). Seasonal circulations in the Malay Peninsula Eastern continental shelf from a wave–tide–circulation coupled model. *Ocean Dyn.* 61, 1317–1328. doi: 10.1007/s10236-011-0432-5

Voris, H. K. (2000). Maps of Pleistocene sea-levels in Southeast Asia: shorelines, river systems and time durations. *J. Biogeogr.* 27, 1153–1167. doi: 10.1046/j.1365-2699.2000.00489.x

Wan, S., Li, A., Clift, P. D., and Stuut, J. B. W. (2007). Development of the East Asian monsoon: mineralogical and sedimentologic records in the northern South China Sea since 20 Ma. *Palaeogeogr. Palaeoclimatol. Palaeoecol.* 254, 561–582. doi: 10.1016/j.palaeo.2007.07.009

Wan, S., Toucanne, S., Clift, P. D., Zhao, D., Bayon, G., Yu, Z., et al. (2015). Human impact overwhelms long-term climate control of weathering and erosion in southwest China. *Geology* 43, 439–442. doi: 10.1130/G36570.1

Wang, A., Bong, C., Xu, Y., Hassan, M. H. A., Xiang, Y., Bakar, A. F. A., et al. (2017). Assessment of heavy metal pollution in surficial sediments from a tropical river-estuary-shelf system: a case study of Kelantan River, Malaysia. *Mar. Pollut. Bull.* 125, 492–500. doi: 10.1016/j.marpolbul.2017.08.010

Wang, A., Wei, B., Xiang, Y., Li, Y., Hassan, M. H. A., Hoe, L. K., et al. (2020). Transport mechanism and fate of terrestrial materials delivered by a small tropical mountainous river: a case study of the Kelantan River, Malaysia. *Mar. Geol.* 430:106344. doi: 10.1016/j.margeo.2020.106344

Wang, H., Liu, Z., Sathiamurthy, E., Colin, C., Li, J., and Zhao, Y. L. (2011). Chemical weathering in Malay Peninsula and North Borneo: clay mineralogy and element geochemistry of river surface sediments. *Sci. China Earth Sci.* 54, 272–282. doi: 10.1007/s11430-010-4158-x

Wang, P., Clemens, S., Beaufort, L., Braconnot, P., Ganssen, G., Jian, Z., et al. (2005). Evolution and variability of the Asian monsoon system: state of the art and outstanding issues. *Quat. Sci. Rev.* 24, 595–629. doi: 10.1016/j.quascirev.2004.10.002

Wei, G., Liu, Y., Li, X., Shao, L., and Fang, D. (2004). Major and trace element variations of the sediments at ODP Site 1144, South China Sea, during the last 230 ka and their paleoclimate implications. *Palaeogeogr.*

Palaeoclimatol. Palaeoecol. 212, 331–342. doi: 10.1016/j.palaeo.2004.06.011

Wei, G., Liu, Y., Ma, J., Xie, L., Chen, J., Deng, W., et al. (2012). Nd, Sr isotopes and elemental geochemistry of surface sediments from the South China Sea: implications for provenance tracing. *Mar. Geol.* 319, 21–34. doi: 10.1016/j.margeo.2012.05.007

West, A. J., Galy, A., and Bickle, M. (2005). Tectonic and climatic controls on silicate weathering. *Earth Planet. Sci. Lett.* 235, 211–228. doi: 10.1016/j.epsl.2005.03.020

White, A. F., and Blum, A. E. (1995). Effects of climate on chemical weathering in watersheds. *Geochim. Cosmochim. Acta* 59, 1729–1747. doi: 10.1016/0016-7037(95)00078-E

Wu, K., Liu, S., Kandasamy, S., Jin, A., Lou, Z., Li, J., et al. (2019). Grain-size effect on rare earth elements in Pahang River and Kelantan River, Peninsular Malaysia: implications for sediment provenance in the southern South China Sea. *Cont. Shelf Res.* 189:103977. doi: 10.1016/j.csr.2019.103977

Wu, K., Liu, S., Shi, X., Lou, Z., Kandasamy, S., Wu, B., et al. (2020). Distribution of rare earth elements in surface sediments of the western Sunda Shelf: constraints from sedimentology and mineralogy. *Cont. Shelf Res.* 206:104198. doi: 10.1016/j.csr.2020.104198

Xue, Z., He, R., Liu, J., and Warner, J. C. (2012). Modeling transport and deposition of the Mekong River sediment. *Cont. Shelf Res.* 37, 66–78. doi: 10.1016/j.csr.2012.02.010

Xue, Z., Liu, J., DeMaster, D., Van Nguyen, L., and Ta, T. K. O. (2010). Late Holocene evolution of the Mekong subaqueous delta, southern Vietnam. *Mar. Geol.* 269, 46–60. doi: 10.1016/j.margeo.2009.12.005

Zong, Y., Huang, K., Yu, F., Zheng, Z., Switzer, A. D., Huang, G., et al. (2012). The role of sea-level rise, monsoonal discharge and the palaeo-landscape in the early Holocene evolution of the Pearl River delta, southern China. *Quat. Sci. Rev.* 54, 77–88. doi: 10.1016/j.quascirev.2012.01.002

Conflict of Interest: The authors declare that the research was conducted in the absence of any commercial or financial relationships that could be construed as a potential conflict of interest.

The handling editor declared a past co-authorship with one of the authors XS.